Spatiotemporal patterns in simple reaction cell arrays with time delay

ARTICLE *in* THE JOURNAL OF PHYSICAL CHEMISTRY · APRIL 1994

Impact Factor: 2.78 · DOI: 10.1021/j100065a028

Spatiotemporal Patterns in Simple Reaction Cell Arrays with Time Delay

M. Dolník, J. Kosek, V. Votrubová, and M. Marek*

Department of Chemical Engineering, Prague Institute of Chemical Technology, Technická 5, 166 28 Prague 6, Czech Republic

Received: May 24, 1993; In Final Form: October 25, 1993®

The effects of the intensity of coupling and the time delay on the properties of circulating spatiotemporal firing patterns in several simple cell arrays have been studied for the Belousov–Zhabotinskii (BZ) and chlorine dioxide–iodide reaction kinetics models. Single firing and finite cascade of firings have been found for both systems, but permanent firing has been observed only in the Oregonator model of the BZ reaction. The existence of regimes with permanent firing have been explained on the basis of the difference in the course of concentration trajectories of the studied systems.

1. Introduction

Propagation of impulses in the form of pulse waves is a common feature in active (excitable, conducting) tissues in neuro- and cardiophysiology.[1] They are discrete, consisting of cells (compartments) mutually coupled via electrical and/or mass exchange (chemical) contacts. Circulating waves are of special importance, particularly in myocardial and brain tissue. For example, the recent results of PET scanning show that working memory is located in the prefrontal cortex. Working memories are retained by the continuous activity of particular neurons. These neurons stimulate themselves either directly or via a loop involving others. When they stop firing, the memory is lost unless it has been passed on to the hippocampus for more permanent storage.[2,3]

In this paper we study the conditions of existence and properties of circulating excitations (firings) in several compartmentalized chemical systems. We concentrate our attention on the effects of intensity of mass coupling and the time delay on the properties of simple circulating spatiotemporal firing patterns. We compare the behavior of two popular excitable chemical systems—the Belousov–Zhabotinski (BZ) reaction and the chlorine dioxide–iodine reaction, which differ in their response to stimulation.

Compartmental chemical systems are now relatively well understood from the point of view of agreement between experimental observations and simulations based on robust mathematical models, after more than 25 years of research. Studies of model chemical compartmentalized systems have been at first only theoretical. Thus Prigogine and Lefever have studied two coupled cells.[4] Scriven and Othmer[5] and Martinez and Baer[6] have analyzed the stability properties of arbitrary network of compartments, mostly by analytical methods. Bunow and Colton[7] have studied the behavior of a linear array of cells with enzymatic reaction with substrate-inhibited kinetics. They have found asymmetric steady-state concentration profiles.

Two coupled continuous stirred tank reactors (CSTRs) with mutual mass exchange and oscillatory Belousov–Zhabotinski (BZ) reaction have been first studied experimentally in 1975.[8] Later, asymmetric steady-state concentration patterns and their stability have been investigated in a hexagonal structure of seven reactors (CSTRs) with mutual mass exchange.[9] Two coupled CSTRs with an oscillatory reaction and direct mass exchange were also studied experimentally by Sawada and co-workers.[10,11] Two CSTRs coupled electrically were investigated by Crowley and Field.[12] Crowley and Epstein[13] and Dolník et al.[14] have studied experimentally the oscillatory behavior of the BZ reaction in two coupled CSTRs with mutual mass exchange. Breton et al.[15] and Marmillot et al.[16] have studied experimentally multiple steady states in two and three coupled CSTRs with mutual diffusional coupling. They have used a photobiochemical reaction catalyzed by immobilized thylakoids and demonstrated both experimentally and on numerically solved models the occurrence of both stable symmetric and asymmetric steady states in a circular and linear array of cells. Laplante and Erneux[17] have built a one-dimensional array of 16 coupled stirred tank reactors. They have used the bistable chlorite–iodide reaction and investigated propagation of the front wave in the system. Weiner et al.[18] studied two identical chemical oscillators (minimal bromate oscillator) coupled by means of the mutual regulation of the flow rate of one reactor by the output of the other and vice versa according to measured Ce^{4+} ion concentration with defined time delay and intensity of coupling. The minimal bromate oscillator in single cell with delayed feedback were studied earlier experimentally also by Weiner et al.[19] Dolník and Epstein[20] have described the bursting behavior of the chlorine dioxide–iodide reaction in two CSTRs coupled by reciprocally regulated mass inflow. Kosek and Marek[21] have studied experimentally propagation of excitation in two continuous stirred tank reactor cells mutually coupled via direct mass exchange through the common wall and modeled the propagation of excitation in a linear array of N-coupled cells via the Oregonator model.

Raschman et al.[22] have studied periodic and aperiodic regimes in linear and cyclic arrays of coupled cells with mutual mass exchange and Brusselator kinetics. Hunt et al.[23] investigated the relative stability of coupled reactors with a system with multiple stationary states. Theoretical and computational studies in coupled cells are numerous and have been recently reviewed in two book publications.[24,25] A review of chaotic regimes in coupled and forced excitable and oscillatory cells has been also published recently.[26] Computational properties of the system of mass coupled CSTRs and modeling properties of neural networks were also studied recently.[27]

In the above listed experimental studies of coupled cells three ways of the coupling were realized: (a) mass coupling via direct convective–diffusive mass exchange between neighboring cells; (b) electric coupling; (c) mass coupling via pumping between the cells.

These ways of coupling differ in the extent of the time delay in the coupling signal. In case (a) time delay is low, in case (b) the extent of the coupling delay can be controlled (e.g., via computer), and case (c) always includes significant time delay.

Recently we have designed an experimental setup of three flow-through CSTRs with the possibility of using all three above ways of mutual coupling. Hence we should be able to study and compare the effects of time delay introduced by various ways of coupling. In this paper we present first the results of the study of the coupling intensity and the time delay on the propagation of excitations

* Abstract published in *Advance ACS Abstracts*, December 15, 1993.

0022-3654/94/2098-3707$04.50/0

and wavelike spatiotemporal patterns in the excitable Belousov–Zhabotinski (BZ) reaction modeled by the Oregonator model and then the results for the chlorine dioxide–iodide reaction also modeled by a simple three-dimensional model. We believe that both experimental and connected modeling studies of circulating chemical waves under relatively well-defined conditions can be of importance in the understanding of circulating patterns in general and also help in an interpretations in biological systems, particularly in both chemical and electric synapse.

2. Models of Arrays of Reaction-Transport Coupled Cells with Time Delay

A sketch of a group of synapses according to ref 28 is shown in Figure 1a. The modeled systems of coupled cells studied in this paper are schematically shown in Figure 1b.

Let us consider a linear or cyclic array of cells. Each cell can exchange mass with both the environment and with its neighbors. Mass balances for the system of N coupled cells with n reaction components may be written in the form

$$dc_i^k/dt = f_i(c_1^k, ..., c_n^k) + d_i\sum_{l=1}^{N}\delta^{lk}(c_i^l(t-\tau) - c_i^k(t)) \quad (1)$$

Here c_i^k is the concentration of the ith reaction component in the kth cell, f_i: $\mathbf{R}^n \rightarrow \mathbf{R}$ are functions describing reaction kinetics and mass exchange with the environment. The rate of transport of the ith component between the cells is proportional to the difference between the concentrations $c_i^l(t-\tau)$ and $c_i^k(t)$, where τ denotes the time-delay in the concentration of the component i exchanged between the lth and the kth cells, respectively. Here $\delta^{lk} = 1$ when the connection from l to k exists, otherwise $\delta^{lk} = 0$. The values $d_1, ..., d_n$ have been set in calculations to the same value $k_x = d_1 = ... = d_n$, where k_x denotes mass-transport coefficient between cells. In this study the reactions outside the reactors were omitted.

3. Numerical Method

Numerical integration of a nonautonomous system of ODEs can be a computer-time-consuming task, particularly if the dimension of the system increases. We have used the modified semiimplicit Runge–Kutta type fourth order method with an automatic control of the step length. The original nonautonomous system of eqs (1), $d\mathbf{p}/dt = f(\mathbf{p},t)$ ($\mathbf{p}$ is a vector of state variables and t denotes time), has been transformed into an autonomous system:

$$d\mathbf{p}/ds = f(\mathbf{p},t) \qquad dt/ds = 1 \quad (2)$$

The values of t, $\mathbf{p}$, and $d\mathbf{p}/dt$ were after each integration step added into a shifting queue (stack) of saved values. The values of $\mathbf{p}(t-\tau)$ (τ denotes time delay) were then obtained from the course of the queue of saved values in the proper neighborhood of the point $(t-\tau)$. The elements of the Jacobi matrix of the system have been evaluated as

$$dp_i(t-\tau)/dp_i = (dp_i(t-\tau)/dt)/(dp_i/dt) \quad (3)$$

where the values of $dp_i(t-\tau)/dt$ were also obtained by a Lagrange interpolation from the shifting queue of saved values.

4. Oregonator Model

The well-known Oregonator model of the BZ reaction[29] have been used in the form

$$f_1(X,Y,Z) = k_1BY - k_2XY + k_3BX - 2k_4X^2 + k_0(X_0 - X) \quad (4)$$

$$f_2(X,Y,Z) = -k_1BY - k_2XY + fk_5Z + k_0(Y_0 - Y) \quad (5)$$

$$f_3(X,Y,Z) = k_3BX - k_5Z + k_0(Z_0 - Z) \quad (6)$$

TABLE 1: Oregonator Parameter Values[a]

parameter	simulation with FKN values	simulation with FF values
k_1	2.00 dm^3 mol^{-1} s^{-1}	$2 \times [H^+]^2$ dm^3 mol^{-1} s^{-1}
k_2	2×10^9 dm^3 mol^{-1} s^{-1}	$3 \times 10^6 \times [H^+]$ dm^3 mol^{-1} s^{-1}
k_3	1×10^4 dm^3 mol^{-1} s^{-1}	$42 \times [H^+]$ dm^3 mol^{-1} s^{-1}
k_4	5×10^7 dm^3 mol^{-1} s^{-1}	3×10^3 dm^3 mol^{-1} s^{-1}
k_5	1.00	$1 \times$ MA s^{-1}
X_0	0.00 mol dm^{-3}	0.00 mol dm^{-3}
Y_0	1×10^{-6} mol dm^{-3}	1×10^{-2} mol dm^{-3}
Z_0	1×10^{-3} mol dm^{-3}	6×10^{-3} mol dm^{-3}
B	0.10 mol dm^{-3}	0.10 mol dm^{-3}
f	1.00	1.00
$[H^+]$		0.82 mol dm^{-3}
MA		0.10 mol dm^{-3}

[a] The sets of rate constants labeled by FKN and FF are those suggested by Field, Körös, and Noyes[30] and by Field and Försterling,[31] respectively. The values of input concentrations were taken in the case FKN from our previous modeling, cf. ref 21, and in the case FF the real concentrations from our experiments with excitable cells were used.

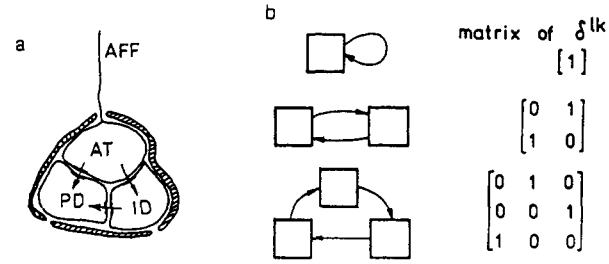

Figure 1. (a) Group of synapses; cf. ref 28. AFF, afferent axon; AT, synapse of external axon; PD, dendrite of principal neuron; ID, dendrite of intrinsic neuron. (b) Configurations studied in this paper.

where X denotes the concentration of HBrO_2, Y the concentration of Br^-, Z the concentration of Ce^{4+}, and B the concentration of BrO_3^-, respectively. Two sets of the parameters were used for calculations; cf. Table 1. In the first set the values of the parameters used in the modeling of excitation propagation in two coupled cells[21] based on the FKN constants[30] have been used also in this study. The results obtained with these parameters have been compared with the results with the FF rate constants[31] considering concentrations used in experiments.[21]

4.1. Firing Patterns in the Oregonator Model. *4.1.1. Single Reaction Cell with Delayed Feedback.* The most simple model of a reaction cell (an enclosure, cell compartment, a neuron synapse, etc.) can be represented by a single continuously stirred reactor with a delayed feedback; cf. Figure 1b. We shall study the response of such a reactor to a single superthreshold concentration stimulation with an amplitude A. In the Oregonator model we consider that the amplitude $A < 0$ as we assume that the perturbation corresponds to a decrease of the concentration of Br^- ions caused by an addition of Ag^+ ions into the reactor, cf. experimental procedure and results in ref 21.

Global simulation study of the single reactor for values of parameters describing an excitable regime in the reactor has revealed the following types of the behavior (firing patterns):

Pattern A_s: A single excitation (firing) occurs in the cell; cf. Figure 2a–c. We can observe in the figure that single full-amplitude excitation occurs and then the excitations decay relatively fast. The successful firing can be identified on the basis of the time course of Ce^{4+} or Br^- ions (proportional to redox potential changes), similar to that in ref 21.

Pattern B_s: A finite cascade of firings, with the firing number n occurs; cf. Figure 2d. It means that the reactor is able to self-excite and the period of firings (self-excitations) is determined by the value of the time delay.

Pattern C_s: Permanent firing. For sufficiently large value of the time delay the cell can self-excite continuously ($n = \infty$); cf.

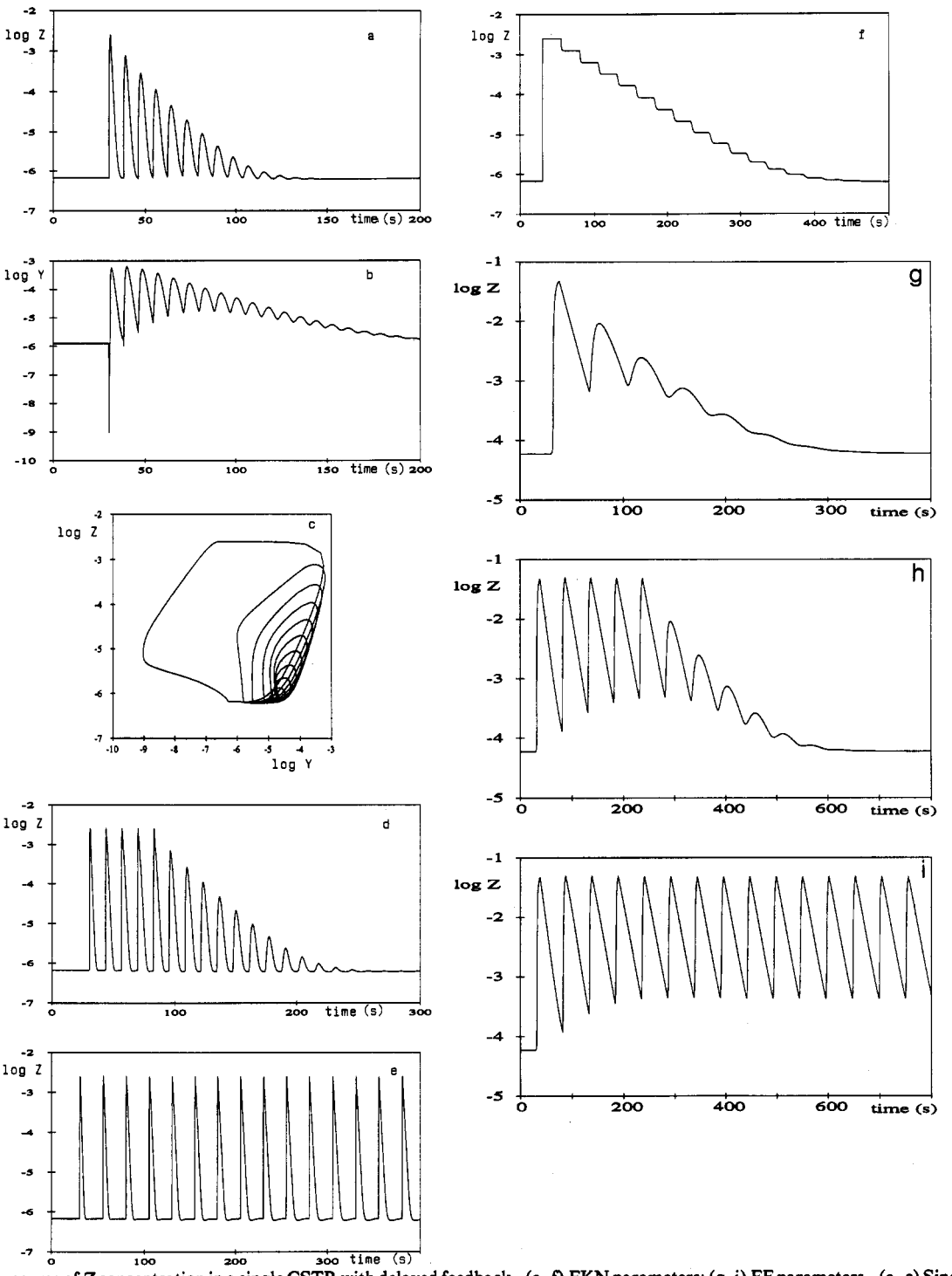

Figure 2. Time course of Z concentration in a single CSTR with delayed feedback. (a–f) FKN parameters; (g–i) FF parameters. (a–c) Single successful excitation, pattern A_s; $k_x = 0.90\ s^{-1}$, $\tau = 8.0$ s, $A = -0.75 \times 10^{-6}$ M. (a) log $Z(t)$, (b) log $Y(t)$, (c) log $Z(t)$ vs log $Y(t)$. (d) Five successful excitations, pattern B_s; $k_x = 0.90\ s^{-1}$, $\tau = 13.0$ s, $A = -0.75 \times 10^{-6}$ M. log $Z(t)$. (e) Continuous firing pattern C_s; $k_x = 0.90\ s^{-1}$, $\tau = 25.0$ s, $A = -0.75 \times 10^{-6}$ M. log $Z(t)$. (f) Mass-transport driven regime: very slow single excitation pattern D; $k_x = 1.20\ s^{-1}$, $\tau = 25.0$ s, $A = -0.75 \times 10^{-6}$ M. log $Z(t)$. (g) Single successful excitation, pattern A_s; $k_x = 0.05\ s^{-1}$, $\tau = 35.0$ s, $A = -0.60 \times 10^{-5}$ M. log $Z(t)$. (h) Five successful excitations, pattern B_s; $k_x = 0.05\ s^{-1}$, $\tau = 49.0$ s, $A = -0.60 \times 10^{-5}$ M. log $Z(t)$. (i) Continuous firing pattern C_s; $k_x = 0.05\ s^{-1}$, $\tau = 50.0$ s, $A = -0.60 \times 10^{-5}$ M. log $Z(t)$.

Figure 2e. This situation is analogous to periodically stimulated single CSTR without a time delay with superthreshold amplitude of the stimulation and the period of stimulation $T > T_R$ (T_R is a refractory period); cf. 32.

Pattern D: When the feedback flow (the value of the parameter k_x) increases, it becomes a controlling process. The excitation is overwhelmed by the feedback flow and a slowly decaying return to the steady state in the reactor can be observed; cf. Figure 2f.

We have used here for the patterns A, B, C a subscript s, which indicates simple excitations. Later in the text we use a subscript c for complex excitations.

With the set of FF parameter values we obtained qualitatively the same results. The examples of patterns A_s, B_s, and C_s for the FF parameter set are depicted on Figure 2g–i. For both sets of parameters we can compare the differences between the input and maximal concentrations of Ce^{4+}. These differences are caused by the missing stoichiometric constraint and by the missing rate expressions connecting the concentrations of Ce^{4+} and Ce^{3+} in the used model.

4.1.2. Cell Arrays. The behavior described above (patterns A_s–D) are in principle preserved in cyclic cell arrays. However, the excitation will not propagate for lower values of the mutual

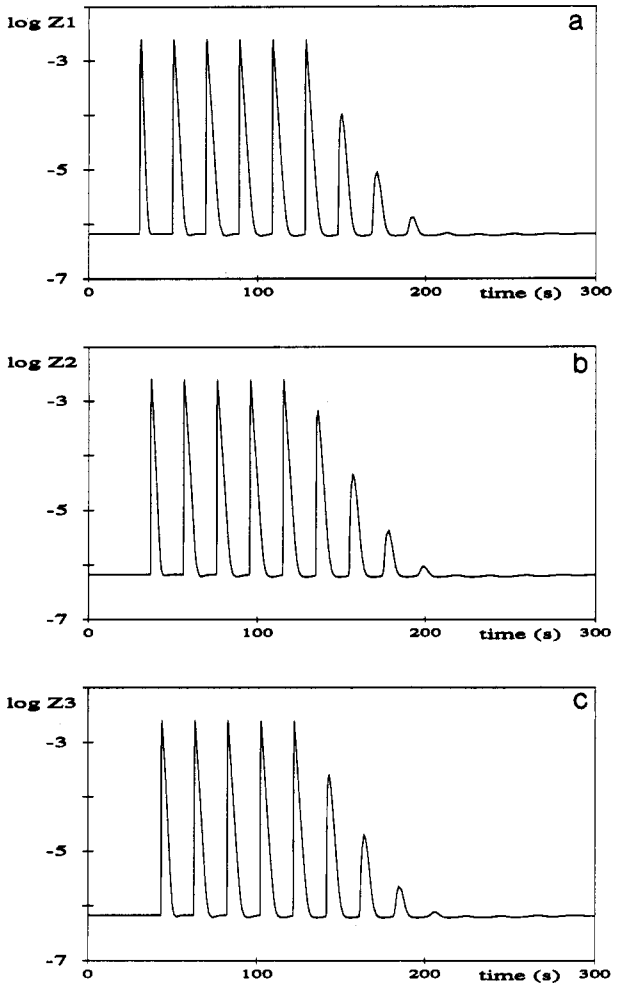

Figure 3. Time course of Z concentrations in a cyclic array of three CSTRs with a delayed mass exchange, FKN parameters, $A = -0.75 \times 10^{-6}$ M, $k_x = 0.90$ s^{-1}, $\tau = 6.5$ s, pattern B_s. (a) log $Z_1(t)$, six successful firings. (b) log $Z_2(t)$, five successful firings. (c) log $Z_3(t)$, five successful firings.

coupling (mass transport) coefficient k_x through entire cascade. Thus an additional type of the pattern (pattern E_s) with the propagation failure of excitations will be also observed.

Pattern E_s: For example, for two reaction cells we observe the pattern where the firing occurs in a single cell only, $n_1 = 1$ and $n_2 = 0$ (n_i denotes the number of firings in the ith cell). This will be denoted as pattern E_s and it has been discussed in detail for two cells in ref 21.

In general, in the cyclic arrays of two and more coupled cells we can observe firing regimes belonging to the pattern B_s, where for two cells either $n_1 = n_2$ or $n_1 = n_2 + 1$, $n_1 > 1$ and in the case of three cells either $n_1 = n_2 = n_3$ or $n_1 = n_2 = n_3 + 1$ or $n_1 = n_2 + 1$ and $n_2 = n_3$; $n_1 > 1$, respectively.

Examples of the time courses of the variable Z for three cells in the case where $n_1 = n_2 + 1 = n_3 + 1 = 6$ are in Figure 3.

The overall dependence of the firing numbers n_1, n_2 in two coupled cells on the time delay is depicted in Figure 4. We can observe the sequence of regimes with increasing values of firing numbers n_1 and n_2 and the existence of a limit value of the time delay τ^* for the permanent firing. For values of time delay $\tau > \tau^*$ two cells mutually stimulate themselves indefinitely, i.e., $n_1 = n_2 = \infty$.

Typical diagrams of computed regimes in the parametric plane mass-transport (coupling) coefficient k_x–time delay τ are given in Figure 5. For high values of k_x we can observe slow decay of single excitation (pattern D). In the region of low values of time delays and intermediate values of k_x a single firing in each cell exists (pattern A_s). When the value of the time delay τ is increased,

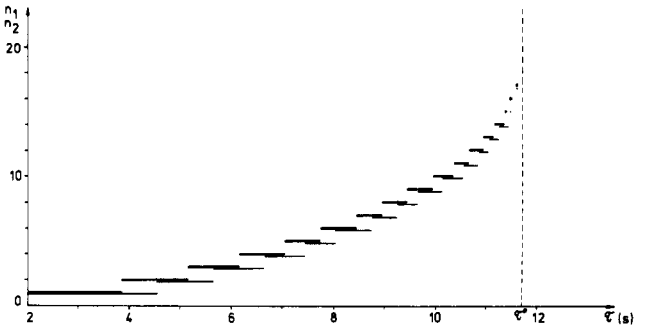

Figure 4. Dependence of the number of firings n_1, n_2 on a time delay τ for two CSTRs with a delayed mass exchange, FKN parameters, $A = -0.8 \times 10^{-6}$, $k_x = 1.00$ s^{-1}.

we subsequently observe regions with finite number of firings (pattern B_s) and finally continuous firing (pattern C_s). In arrays of cells we can observe the presence of the pattern E_s for lower values of k_x.

When Figure 5c,d obtained for different stimulation amplitudes are compared, we observe that when higher absolute value of the stimulation amplitude (A) is used, then the regions of the parameter space with patterns B_s and C_s are located in a narrower range of values of the mass-transport (coupling) coefficient k_x. When even higher stimulation amplitudes are used ($A < -0.86 \times 10^{-6}$ M), then the regions of patterns B_s and C_s disappear from the diagrams. Increase of the amplitude of stimulation in two coupled cells with time delay thus can cause a failure in the propagation of firings. Hence we can observe a qualitatively similar type of the propagation failure as reported earlier in experimental study of two coupled excitable cells.[21]

We can also compare Figure 5a,b to illustrate the effect of used rate constants. The forms of the diagrams on these figures are qualitatively the same. In the case of the FKN parameters we can observe that, for example, for the continuous firing pattern shown in Figure 2e, the values of k_x correspond to 22.5 volumes of the reactor present in the feedback. In the case of the FF parameters the volume of the solution outside the reactor is smaller, e.g., for the same pattern C_s shown in Figure 2i there are only 2.5 volumes contained in the feedback. The values of the mass transport coefficients k_x in these figures are still relatively large when compared with the value of the flow rate $k_0 = 5 \times 10^{-4}$ s^{-1}. However, we can interpret the high values of the volume of reacting mixture contained in the recycle also in such a way that reactions take place only within the reactor (photoreaction activated by illumination of the reactor, immobilized enzyme, or catalyst with high turnover numbers localized in the reactor) and then the ratios of the recycled volumes to actual reaction volume are common. This is also true in biological systems (high perfusion rates). The systems with a small localized reaction center (e.g., immobilized enzymes or solid catalysts) and with a large amount of the reaction mixture circulating through that reaction center possess also another property of our model: reaction mixture does not react outside the reactor.

The results for two or three coupled reactors with the FF parameters do not exhibit any new phenomena. In the case of the FF parameters we did not observe the dependence of the location of the regimes in the parametric plane "mass transport coefficient k_x–time delay" τ on the amplitude of the stimulation (for superthreshold stimulations).

5. Model of the Chlorine Dioxide–Iodide Reaction

The model used for chlorine dioxide–iodide reaction is based on two overall stoichiometric reactions:

$$2ClO_2 + 2I^- \rightarrow I_2 + 2ClO_2^- \quad (7)$$

$$ClO_2^- + 4I^- + 4H^+ \rightarrow Cl^- + 2I_2 + 2H_2O \quad (8)$$

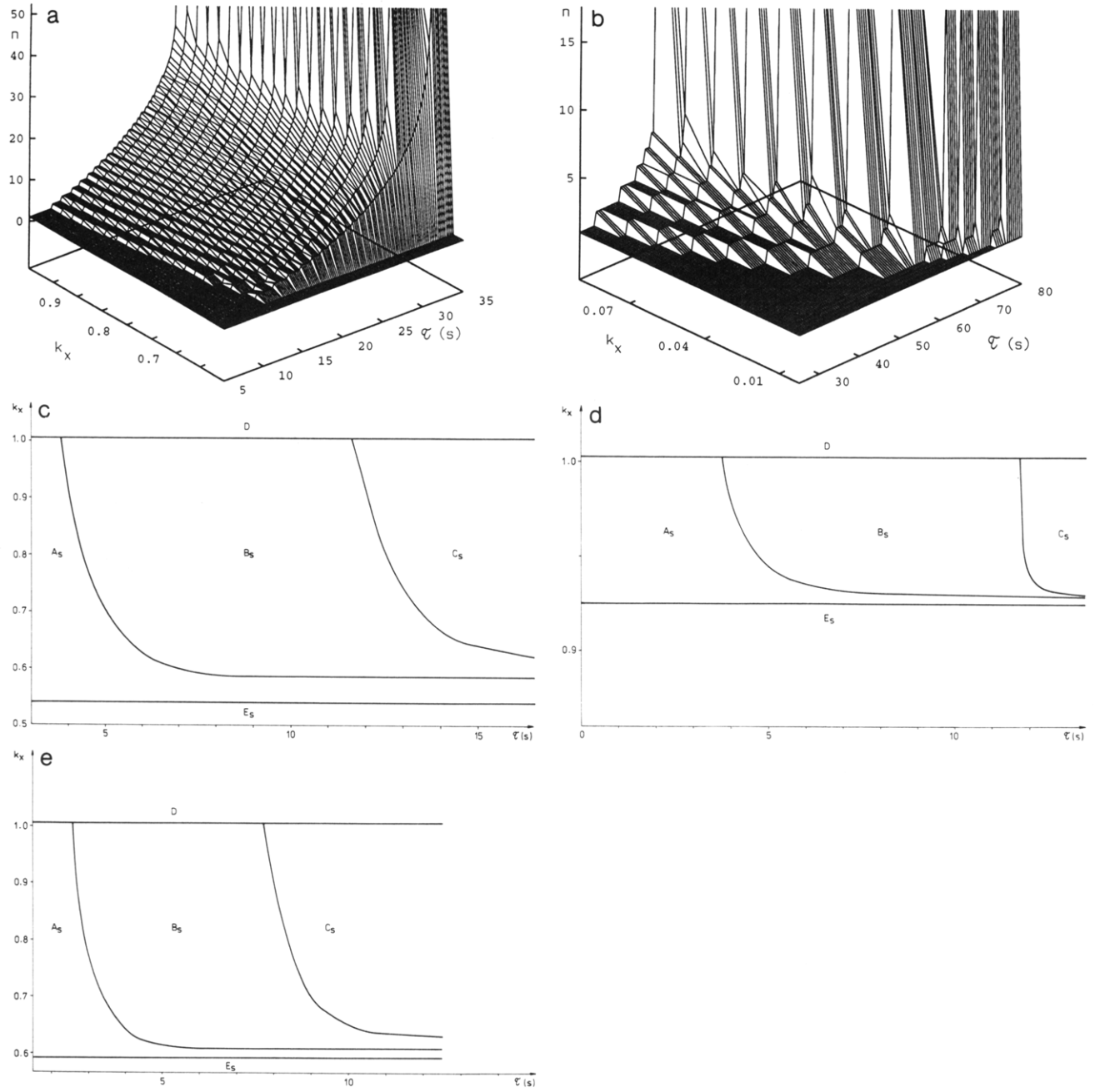

Figure 5. Various firing regimes in the plane mass-transport coefficient k_x, time delay τ. A_s, single firing in each cell; B_s, multiple firings in each cell; C_s, continuous firing; D, mass-transport driven regime—single slow excitation; E_s, single excitation in the stimulated reactor. (a) Single CSTR with a delayed feedback, on vertical axis is number of excitations, FKN parameters, $A = -0.75 \times 10^{-6}$ M. (b) Single CSTR with a delayed feedback; on the vertical axis is the number of excitations, FF parameters, $A = -0.60 \times 10^{-5}$ M. (c) Two CSTRs with a delayed mutual mass exchange, FKN parameters, $A = -0.75 \times 10^{-6}$ M. (d) Two CSTRs with a delayed mutual mass exchange, FKN parameters, $A = -0.80 \times 10^{-6}$ M. (e) Cyclic array of three CSTRs with a delayed mass exchange, FKN parameters, $A = -0.75 \times 10^{-6}$ M.

with the rate laws[33]

$$R_1 = k_1XY \tag{9}$$

$$R_2 = k_{2a}ZYH + k_{2b}ZPY/(u + Y^2) \tag{10}$$

where $X = [ClO_2]$, $Y = [I^-]$, $Z = [ClO_2^-]$, $P = [I_2]$, $H = [H^+]$, and u is a phenomenological parameter.

As far as the entire sum of iodine-containing species in the system is constant, the iodine concentration in the CSTR can be calculated from the iodide concentration:[34]

$$P = (Y_0 - Y)/2 \tag{11}$$

and the model can then be written in the form

$$f_1(X,Y,Z) = -R_1 + k_0(X_0 - X) \tag{12}$$

$$F_2(X,Y,Z) = -R_1 - 4R_2 + k_0(Y_0 - Y) \tag{13}$$

$$f_3(X,Y,Z) = R_1 - R_2 + k_0(Z_0 - Z) \tag{14}$$

where k_0 is a reciprocal value of the residence time and the subscript 0 represents input concentrations. The values of the parameters used in the simulation are shown in Table 2.

5.1. Patterns in the Model of ClO_2–I^- Reaction. *5.1.1. Single Reaction Cell.* The study of the pulse stimulations of the reaction in a single reactor cell is described in ref 35. In this paper we have chosen the stimulation by chlorite ions (variable Z). For an excitable regime a response to a superthreshold stimulation

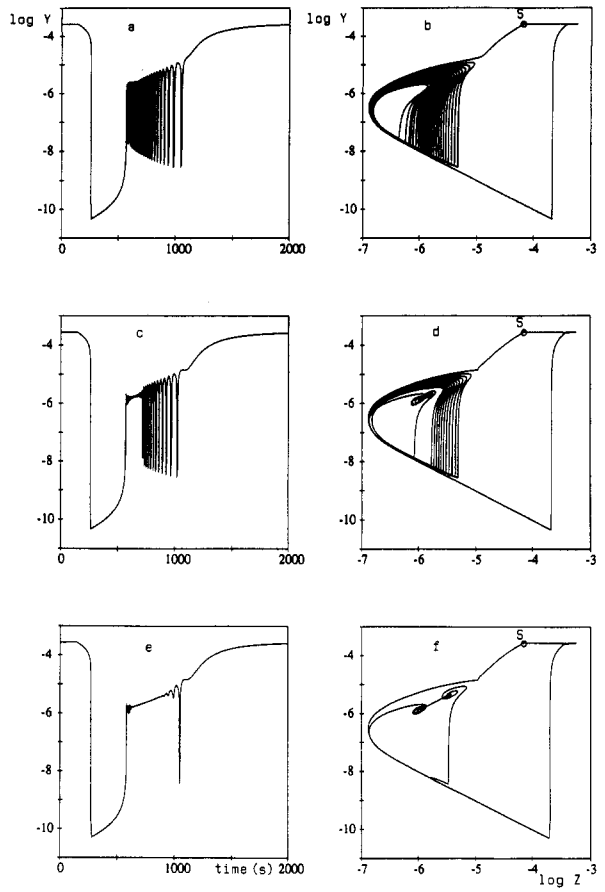

Figure 6. Time course and 2D phase plane for a single CSTR with the chlorine dioxide–iodide reaction with delayed feedback, single complex excitations pattern A_c, $A = 5 \times 10^{-4}$ M, $k_x = 0.15$ s^{-1}. (a, b) $\tau = 3.5$ s, 26 oscillations. (c, d) $\tau = 3.7$ s, 13 oscillations. (e, f) = 4.1 s, 2 oscillations.

TABLE 2: Values for Model of the Chlorine Dioxide–Iodide Reaction

parameter	value	parameter	value
k_1	600 dm^3 mol^{-1} s^{-1}	X_0	1×10^{-4} mol dm^{-3}
k_{2a}	460 dm^6 mol^{-2} s^{-1}	Y_0	5×10^{-4} mol dm^{-3}
k_{2b}	2.55×10^{-3} s^{-1}	Z_0	0.00 mol dm^{-3}
u	1×10^{-14} mol^2 dm^{-6}	H	0.01 mol dm^{-3}
k_0	5×10^{-4} s^{-1}		

is represented by a sequence of temporal oscillations after which the state of the system returns back to the steady state (cf. Figure 6a). The number of oscillations m excited by a single-pulse stimulation depends on the amplitude of stimulation A, the inlet concentrations and the flow rate. In the single cell with the delayed feedback the number of oscillations can be further affected by the coefficient of mass coupling k_x and by the value of the time delay τ (see Figure 7).

If the amplitude of the stimulation is slightly above its superthreshold value, then the surface representing the dependence of the number of oscillations on the mass coupling and on the time delay has monotonic shape as shown in Figure 7a. For values of $k_x \to 0$, the system behaves as a simple single cell and the number of oscillations is determined by the amplitude of stimulation for given reaction conditions. Also, for a small value of the mass coupling k_x, the time delay has almost no effect. But for intermediate values of k_x (3×10^{-3} s$^{-1} < k_x < 1 \times 10^{-1}$ s^{-1}) the time delay plays an important role. For small values of τ the cell still exhibits the excitable response, but for higher values of τ there is no excitation. In addition, for high values of $k_x > 1 \times 10^{-1}$ the stimulation ceases to be a superthreshold one. This phenomenon can be explained by the effect of the delayed feedback flow. If this flow is high enough, then the stimulation is "diluted"

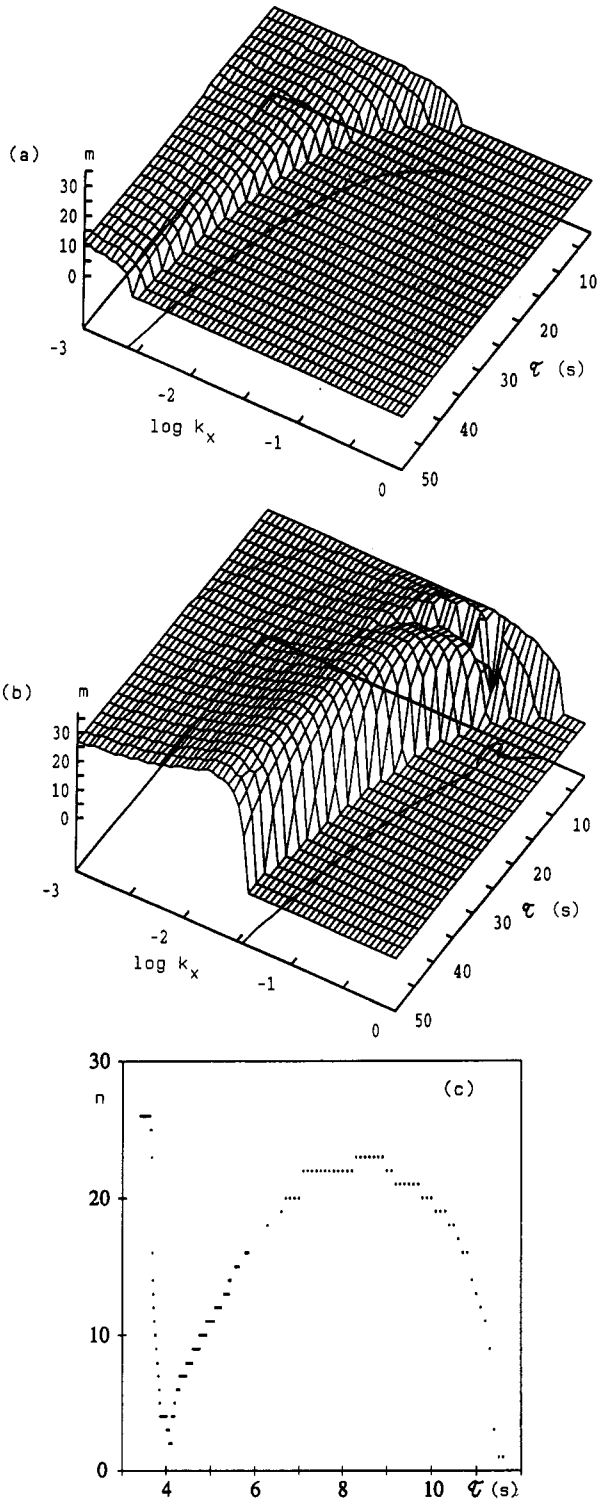

Figure 7. Complex response in the single cell with delayed feedback: the dependence of the number of oscillation on the time delay τ and on the logarithmic value of the mass coupling k_x. (a) Amplitude of stimulation $A = 2 \times 10^{-4}$ M. (b) $A = 5 \times 10^{-4}$ M. $A = 5 \times 10^{-4}$ M, $k_x = 0.15$ s^{-1}.

by the feedback flow and such stimulation then can become a subthreshold one.

For higher amplitudes of the stimulation and for the intensity of the mass coupling very small or very high the effect of the time delay is basically the same as described above (see Figure 7b). However, for intermediate values of k_x a rather different behavior has been observed for stronger stimulations. An extreme (minimum) in the dependence of m on τ has been found (cf. Figure 7c). The time course of oscillations and the phase plane shown in Figure 6c–f illustrates this phenomenon. Because of the delayed feedback the oscillations are suppressed and/or

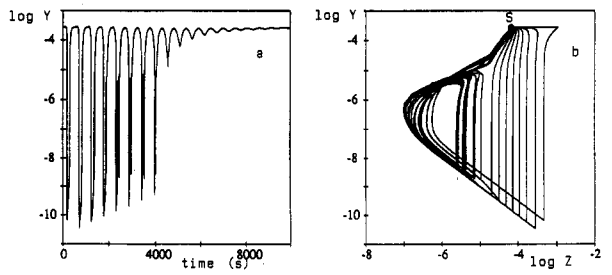

Figure 8. Limited propagation of an excitation in the single cell with delayed feedback, pattern B_c. $A = 1 \times 10^{-3}$ M, $k_x = 0.02$ s^{-1}, $\tau = 500$ s. Eight successful complex firings.

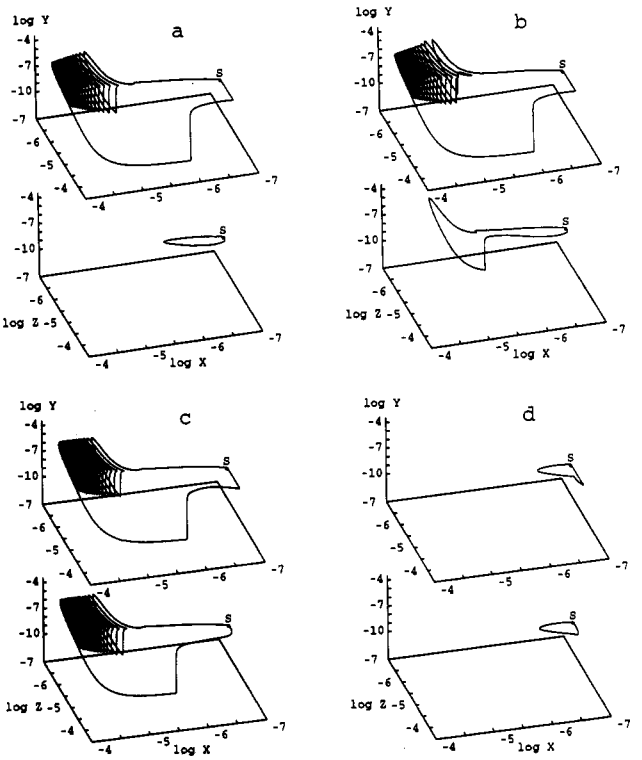

Figure 9. 3D phase phase plane in a array of two CSTRs with chlorine dioxide–iodide reaction with delayed coupling. Upper part, the atractor for cell 1; lower part, cell 2. S, steady state, $A = 5 \times 10^{-4}$ M, $\tau = 10$ s. (a) $k_x = 2.52 \times 10^{-3}$ s^{-1}. (b) $k_x = 2.525 \times 10^{-3}$ s^{-1}. (c) $k_x = 1 \times 10^{-2}$ s^{-1}. (d) $k_x = 4.2 \times 10^{-2}$ s^{-1}.

extinction of oscillations or small-amplitude oscillations occur. The number of oscillations m was evaluated as a number of crossings of a defined surface in the phase space. This surface has been chosen in such a way that the small oscillations (the amplitude of oscillations for any variable is less than 1 order of its magnitude) were not counted. Figure 6e,f corresponds to the minimum on the curve with only two oscillations. This behavior persists for higher amplitudes of the stimulation. As follows from numerical experiments, only the response with a higher frequency of temporal oscillations which is caused by larger stimulations can be suppressed in the presence of the time delay. Hence, a relationship between the frequency of suppressed oscillations and the time delay exists. The time delay for the minimum number of oscillations is approximately equal to one-half of the smallest period of oscillations. The interacting oscillations are just in antiphase, and this is probably the reason the oscillations are suppressed.

In cases with relatively very large time delays repetitive firing patterns can be thus observed. This patterns correspond to patterns B_s described for the Oregonator model. An example of the finite cascade of firings consisting both from simple and complex firings is shown in Figure 8. The pattern C_s, unlimited firing, has not been found for this system.

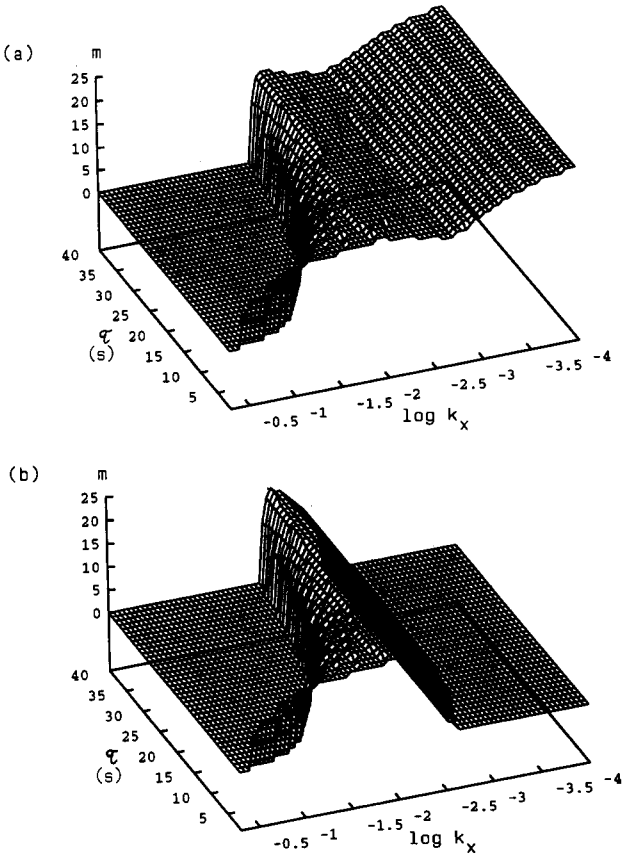

Figure 10. Two CSTRs with delayed mass couplings: the dependence of the number of oscillation m on the time delay τ and on the logarithmic value of the mass coupling k_x, amplitude of stimulation. $A = 5 \times 10^{-4}$ M. (a) Behavior in cell 1. (b) Behavior in cell 2.

5.1.2. Cell Arrays. Similarly as for the Oregonator model the types of behavior found for a single cell with delayed feedback can be observed for cyclic cell arrays.

Examples of the behavior in a two-cell array are depicted in Figure 9. The atractors for both cells are shown for constant time delay for several values of mass coupling. For low values of the mass coupling the firing is excited only in cell 1 (cf. Figure 9a), while cell 2 is not excited. With the increasing value of k_x the simple excitation in the cell 2 can be obtained (cf. Figure 9b) and this simple excitation with the increasing value of k_x gradually alters into a complex excitation with an increasing number of oscillations until the regimes in both reaction cells display the same behavior with equal number of oscillations m (Figure 9c). If the mass coupling increases further the delayed flow between the cells inhibits the excitation (Figure 9d).

From the shape of the attractor we can determine slow and fast variables. The lowest value of variable X is reached at the steady state. After the stimulation in the Z direction, the value of X increases to its maximum and then the system starts to oscillate in the Y–Z plane while the value of X slowly decreases. When X reaches the "critical" value, the oscillations terminate and the system returns back to the steady state. Hence the variables Y and Z play the role of the fast variables while X is the "slow variable".

Similarly as for the single cell with a delayed feedback, the dependence of the number of oscillations on the time delay and on the mass coupling intensity has been constructed for two cells (cf. Figure 10). To initiate the excitation in cell 2, the mass coupling k_x must be high enough to support the transport of the signal from cell 1. The minimal value of k_x for which the excitation is transported into cell 2 does not change with the increasing time delay (cf. Figure 10). The surface representing the number of the oscillations for cell 1 as function of the time delay and the mass coupling possesses a local minimum which coincides

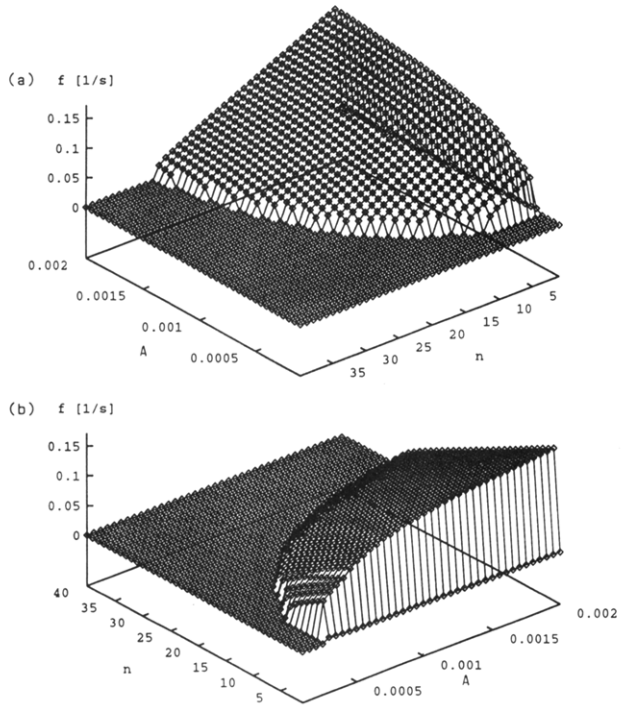

Figure 11. Sequence of frequencies as a function of the amplitude of stimulation: two CSTRs with delayed mass coupling. $A = 5 \times 10^{-4}$ M, $k_x = 3 \times 10^{-3}$ s^{-1}, $\tau = 10$ s.

with this minimal value of k_x. The oscillations in cell 1 are inhibited if there is a flow from the nonexcitatory cell 2. With the increasing value of k_x the inhibition is stronger until the response in cell 2 becomes excitatory. Then the flow between two excited cells supports oscillations and the number of oscillations increases in both cells until the regimes with the same number of oscillations are established in both cells.

We can speculate that a signal which consists of oscillations with changing frequencies is carrying information in the form of the sequence of the frequencies. In Figure 11 is depicted such a sequence as a function of the amplitude of the stimulation.

As example of the limited propagation of complex (bursting) excitations with equal number of firing in each cell $n_1 = n_2 = n_3 = 4$ in three coupled cells is shown in Figure 12. The firing patterns of limited propagation for complex and simple excitation are qualitatively similar. If the cell in which the last firing appeared is cell 3, then the number of firings is equal in all three cells. But if propagation terminates for example in cell 2, the number of firing in cell 3 is smaller by 1 then in cells 1 and 2. The same patterns have been obtained for Oregonator model.

To summarize the behavior in the system with the chlorine dioxide–iodide reaction, we have observed the following types of patterns for the single cell:

Pattern A_c: A single excitation (firing) occurs in the cell. The complex firing was observed and was characterized by the value m, the number of oscillations. The subscript c is used to characterize the complexity of the pattern.

Pattern B_c: A finite cascade of firings; first firings are simple but further become complex, and each firing is formed by a sequence of fast oscillations (bursts). The time delay has to be long enough and comparable with the duration of the single complex response to realize this pattern. The period of firings is determined by the value of the time delay.

Pattern D: When the feedback flow increases, it becomes a controlling process and a nonexcitatory response to the simulation can be observed.

Pattern E_c: For two and more reaction cells the firings can occur in the single cell only. The mass coupling intensity is low to enable a propagation of the excitation into couple cells.

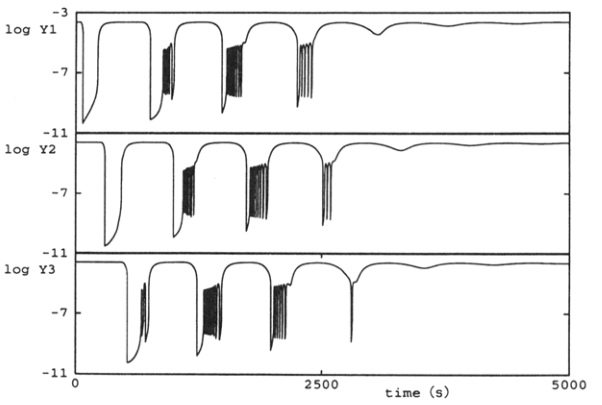

Figure 12. Limited propagation of an excitation in a cyclic array of three cells with delayed coupling: pattern B_c. $A = 1 \times 10^{-3}$M, $k_x = 0.02$ s^{-1}, $\tau = 200$ s.

The only pattern which has not been found in this system is the pattern C_s—continuous firing.

6. Discussion and Conclusions

Generally a single firing (patterns A_s and A_c), a finite cascade of firings (patterns B_s and B_c), a nonexcitatory response (pattern D) in a single cell with the time-delayed feedback, and the patterns E_s and E_c in coupled cells with the firing only in a single cell have been observed for both reactions. However, detailed time courses of individual firing regimes and their representation in the phase space differ significantly for these systems. The regime of permanent firings has been observed only for the Oregonator model. The trajectories for the BZ reaction are generally simpler. More complicated trajectories in the ClO_2–I^- system often appear in the form of bursts with the number of peaks in the single burst depending on the amplitude of the stimulation. Hence the frequency sequences of firings and their information contents are strongly dependent on the type of the nonlinearity in the model, i.e., on the detailed chemical mechanism of the course of the excitation. This situation is similar to the responses to the stimulation of specific chemical synapses in neurophysiology. It is well-known that there have been now identified more than 30 neurotransmitter specific chemical synapses which differ in the characteristic responses to stimulation.

The crucial condition for the existence or nonexistence of permanent firing follows from the behavior of the trajectories in the phase space of concentrations, particularly the time evolution after the stimulation. For the Oregonator model, the system, after stimulation, evolves in such a way that the trajectory moves further away from the threshold boundary (the concentration Y does not reach its extreme just after the excitation). On the other hand, the trajectory calculated for the other model is slowly moving after the stimulation and the concentration of the stimulated variable reaches its maximum value just after the stimulation. Both reactions without any feedback tend to return to the steady state. In the presence of delayed feedback, new excitations can occur. If the feedback is strong enough and the actual state is such that the threshold can be reached, new firing occurs. For the Oregonator model, the time-delayed flow can shift the state of the system further away from the threshold than the first single stimulation. The firings can thus become permanent. In the case of ClO_2–I^- reaction we cannot observe permanent firing because the time-delayed feedback does not shift the state of the system further from the threshold boundary (i.e., the mixture of the solution in the state close to the steady state and in the state the time-delayed flow is in all cases closer to the threshold boundary than the initial stimulation). This distance from the threshold boundary is decreasing with time, and after several firings the threshold is not crossed at all and the firings stop.

Characteristic spatiotemporal patterns may arise in the discrete arrays of coupled cells when a single cell is in an excitable and/or in an oscillatory state. As was illustrated for the case of the Oregonator model, a single stimulation of an excitatory cell can cause excitation of a single pulse, of finite series of pulses, and of infinite circulating series of firings, respectively, in dependence on the amplitude of the stimulation, time delay, and the intensity of coupling. On the contrary, single and finite sequences of complex firings (bursts) can occur in the chlorine dioxide–iodide reaction, but no continuous firings can be observed. Both described types of spatiotemporal patterns can be used under specific conditions for storing information contained in the incoming signal (amplitude of stimulation, a level of the inlet concentration of characteristic component) in the form of a specific firing or spatiotemporal pattern in dependence on the time delay or coupling strength. Simple arrays of cells can be coupled into layers or cellular networks and their computational and learning properties can be studied, similarly as in the case of studies of mass coupled bistable reaction systems; cf. ref 27.

Comparing the results obtained with the FKN and FF parameters, we can conclude that there is no qualitative difference in the observed patterns or in the localization of the regimes in the diagram mass-transport coefficient k_x–time delay τ. The computations with the FF constants do not exhibit some effects observed in our previous experiments with two coupled excitable cells, e.g., propagation failure.[21] On the other hand the Oregonator model with FKN constants displays the propagation failure which was observed in experiments. For this reason we have used also old rate constants, which although incorrect they give better agreement with experiments in this particular study. The magnitude of the mass-transport coefficient k_x used in the simulations with the FKN parameters is of the same order of magnitude as in ref 21, where such a large value was necessary to ensure the propagation of excitation pulse into the unstimulated reactor.

Intact chemoreceptor structures including various nerve cells have been recently coupled to potentiometer electrodes and used as sensors for specific stimulants. Traces of nerve signal responses, in both a single and multiple unit case, are studied quantitatively. Also a development of an integrated ultramicroenzyme sensors (less than 10 μm in diameter), which can be used, for example, for the determination of an important neurotransmitter glutamate,[36] will increasingly enable us to monitor concentrations of active components in living neural systems.[37] These developments make it now possible to study and interpret the behavior of discrete arrays of coupled cells with both relatively well-defined chemical mixtures and still only partly defined chemoreceptor structures in parallel.

Acknowledgment. We thank Pavel Pokorný for software support with the convenient data plotting program.

References and Notes

(1) Holden, A. V.; Markus, M.; Othmer, H. G. *Nonlinear Wave Processes in Excitable Media*; Manchester University Press: Manchester, 1990.
(2) Gelenbe, E. *Neural Networks*; Elsevier: Amsterdam, 1991.
(3) Amit, D. J. *Modeling Brain Functions the World of Attractor Neural Networks*; Cambridge University Press: Cambridge, 1989.
(4) Prigogine, I.; Lefever, R. *J. Chem. Phys.* **1967**, *48*, 1695.
(5) Othmer, H. G.; Scriven, L. E. *J. Theor. Biol.* **1971**, *32*, 507. Othmer, H. G.; Scriven, L. E. *J. Theor. Biol.* **1974**, *43*, 87.
(6) Martinez, H.; Baer, R. M. *Bull. Math. Biol.* **1973**, *35*, 87.
(7) Bunow, B.; Colton, C. K. *Biosystems* **1975**, *7*, 160.
(8) Stuchl, I.; Marek, M. *Biophys. Chem.* **1975**, *3*, 241.
(9) Stuchl, I.; Marek, M. *J. Chem. Phys.* **1982**, *77*, 2956.
(10) Fujii, H.; Sawada, Y. *J. Chem. Phys.* **1978**, *69*, 241.
(11) Nakajimma, K.; Sawada, Y. *J. Phys. Soc. Jpn.* **1981**, *50*, 687. Nakajima, K.; Sawada, Y. *J. Chem. Phys.* **1988**, *72*, 2231.
(12) Crowley, M. F.; Field, R. J. *J. Phys. Chem.* **1986**, *90*, 1907.
(13) Crowley, M. F.; Epstein, I. R. *J. Phys. Chem.* **1989**, *93*, 2496.
(14) Dolník, M.; Padušáková, E.; Marek, M. *J. Phys. Chem.* **1987**, *91*, 4407.
(15) Breton, J.; Thomas, D.; Hervagault, J. F. *Proc. Natl. Acad. Sci. U.S.A.* **1986**, *83*, 551.
(16) Marmillot, P.; Kaufman, M.; Hervagault, J. F. *J. Chem. Phys.* **1991**, *95*, 1206.
(17) Laplante, J. P.; Erneux, T. *J. Phys. Chem.* **1992**, *96*, 4931.
(18) Weiner, J.; Holz, R.; Schneider, F. W.; Bar-Eli, K. *J. Phys. Chem.* **1992**, 496, 8915.
(19) Weiner, J.; Schneider, F. W.; Bar-Eli, K. *J. Phys. Chem.* **1989**, *93*, 2704.
(20) Dolník, M.; Epstein, I. R. *J. Chem. Phys.* **1993**, *98*, 1149.
(21) Kosek, J.; Marek, M. *J. Phys. Chem.* **1993**, *97*, 120.
(22) Raschman, R.; Schreiber, I.; Marek, M. *Lectures in Appl. Math. 24, AMS* **1986**, 81.
(23) Hunt, K. L. C.; Kottalam, J.; Hatlee, M. D.; Ross, J. *J. Chem. Phys.* **1992**, *96*, 7019.
(24) Scott, S. K. *Chemical Chaos*; Clarendon Press: Oxford, 1991.
(25) Marek, M.; Schreiber, I. *Chaotic Behavior of Deterministic Systems*; Academia Publishing House: Prague, and Cambridge University Press: Cambridge, 1991. Second edition, Cambridge University Press: Cambridge, 1993.
(26) Schreiber, I.; Marek, M. Chaos in Forced and Coupled Chemical Oscillators and Excitators. In *Chaos in Chemical and Biological Systems*; Field, R. J., Gyorgyi, Z., Eds.; World Scientific: Singapore, 1993; Chapter 4.
(27) Hjemfelt, A.; Schneider, F. W.; Ross, J. *Science* **1993**, *260*, 335.
(28) Sheperd, G. M. *The Synaptic Organization of the Brain*; Oxford University Press: New York, 1979.
(29) Field, R. J.; Noyes, R. M. *J. Chem. Phys.* **1974**, 460, 1877.
(30) Field, R. J.; Kőrös, E.; Noyes, R. M. *J. Am. Chem. Soc.* **1972**, *94*, 8649.
(31) Field, R. J.; Försterling, H. D. *J. Phys. Chem.* **1986**, *90*, 5400.
(32) Finkeová, J.; Dolník, M.; Hrudka, B.; Marek, M. *J. Phys. Chem.* **1990**, *94*, 4110.
(33) Lengyel, I.; Rabay, G.; Epstein, I. R. *J. Am. Chem. Soc.* **1990**, *112*, 9104.
(34) Lengyel, I.; Li, J.; Epstein, I. R. *J. Phys. Chem.* **1992**, *96*, 7032.
(35) Dolník, M.; Epstein, I. R. *J. Chem. Phys.* **1992**, *97*, 3265.
(36) Tamiya, E.; Sugiura, Y.; Takeuchi, T.; Suzuki, M.; Karube, I.; Akiyama, A. *Sens. Actuators B* **1993**, *10*, 179.
(37) Belli, S. L.; Rechnitz, G. A. *Fresenius Z. Anal. Chem.* **1988**, *331*, 439.